Hydrophobicity in Lennard-Jones solutions

Mario Ishizaki, Hideki Tanaka and Kenichiro Koga*

Received 9th September 2010, Accepted 12th October 2010
DOI: 10.1039/c0cp01767a

The analogue of the hydrophobic hydration is explored for Lennard-Jones solutions. The free energy of solvation and its temperature derivatives, both in the constant-pressure process and in the constant-volume process, are obtained numerically for a variety of the size and energy parameters for the solute–solvent Lennard-Jones potential. We identify in the parameter space a region in which the solvation is of hydrophobic character, with an understanding that hydrophobicity is characterized by both the solvation free energy being positive and the solvation process being exothermic. Such a region is found in each case of the isobaric and isochoric conditions and the region is seen to be much wider in the isochoric process than in the isobaric one. Its origin and implication are discussed.

1. Introduction

The hydrophobic effect is often considered as an essential factor, combined with other effects, for the stability and functionality of proteins and biomembranes in aqueous environments. In a number of review articles and books on water, hydrophobicity is always in the list of characteristic properties of water.[1–3] It is thus natural, and indeed common, in molecular–theoretical attempts to study realistic models of aqueous solutions, from which detailed, experimentally inaccessible information is obtained;[4,5] studying simple models of water, or of solvent in general, is also of high value, for then universal features or important physical implication often obscured by details may be derived from such models.[6–8] Our strategy here is similar in spirit to the latter: we study simple liquid mixtures aiming to examine hydrophobicity from a broader perspective. In particular, we try to identify necessary macroscopic and microscopic conditions that allow solvation of hydrophobic character to be realized in these simple solutions.

An essential feature of the hydrophobicity of nonpolar solutes in water is not the low solubility itself but the fact that it becomes even lower as temperature is increased. The characteristic temperature dependence means that the solvation process in which a solute molecule is transferred from a gas or liquid phase (phase α) to water (phase β) is exothermic: the low solubility comes from some unfavorable entropy change in the solvation process.[9]

The solvation free energy, enthalpy (or energy), and entropy may be defined for the process transferring solute A from phase α to phase β. When it is done with pressure p and temperature T fixed as in the standard experimental condition, the solvation Gibbs free energy is defined by

$$\Delta G_p^* = \Delta G_p - kT \ln(\rho_A^\beta/\rho_A^\alpha), \quad (1)$$

where ΔG_p is the Gibbs free energy change of the composite system (phase α + phase β) in the process, ρ_A^α and ρ_A^β are the number densities of solute molecules in phases α and β, and k is Boltzmann's constant. The point is that the part of ΔG_p that merely comes from the difference in the solute density between two phases, $kT\ln(\rho_A^\beta/\rho_A^\alpha)$, is subtracted from ΔG_p, and so the resulting ΔG_p^* contains essential information on the solvation. Likewise the solvation entropy in the same process is defined by

$$\Delta S_p^* = \Delta S_p + k \ln(\rho_A^\beta/\rho_A^\alpha), \quad (2)$$

where ΔS_p is the entropy change of the composite system. Note that ΔG_p and ΔS_p diverge in the infinite dilution limit ($\rho_A^\beta \to 0$) but ΔG_p^* and ΔS_p^* remain finite. The enthalpy change ΔH_p for the same process is the heat absorbed by the composite system: *e.g.*, the heat is released (*i.e.*, $\Delta H_p < 0$) when a hydrophobic solute is transferred from its own vapor phase to water. The solvation Gibbs free energy is decomposed as

$$\Delta G_p^* = \Delta H_p - T\Delta S_p^*. \quad (3)$$

The hydrophobic hydration is characterized by ΔG_p^* being positive even though ΔH_p is negative, or equivalently

$$\Delta H_p < 0 \text{ and } T\Delta S_p^* < \Delta H_p. \quad (4)$$

The origin of a net release of the heat has long been discussed. A historical view is that the solvation is accompanied by the enhancement of existing hydrogen bonds, or the formation of new hydrogen bonds, between water molecules around a solute.[10] A modern theoretical study, however, indicates that the hydrophobic effect is a result of the unusual equation of state of water.[11] Furthermore a simulation study shows that the hydrophobic effect manifests itself for a model solvent consisting of spherical particles with two characteristic lengths,[12] suggesting that the solvation of hydrophobic character [eqn (4)] may be observed for a larger class of liquid mixtures than naively expected. In fact, as we will see, "hydrophobic" solvation is observed for standard models of liquid mixtures, namely the Lennard-Jones (LJ) fluid mixtures, for certain sets of the interaction parameters. There are earlier studies illustrating that analogues of the hydrophobic interaction are observed for solutes in square-well solvents[13] and Lennard-Jones solvents.[14]

Department of Chemistry, Faculty of Science, Okayama University, Okayama, Japan. E-mail: koga@cc.okayama-u.ac.jp

When the volume, instead of the pressure, of each phase is fixed before and after the transfer of a molecule A, the process is characterized by the solvation Helmholtz free energy ΔA_V^*, energy ΔU_V, and entropy ΔS_V^*, where the subscripts V indicate volume being fixed for the transfer. Definitions of ΔA_V^* and ΔS_V^* are analogous to eqn (1) and (2): $\Delta A_V^* = \Delta A_V - kT\ln(\rho_A^\beta/\rho_A^\alpha)$ and $\Delta S_V^* = \Delta S_V + k\ln(\rho_A^\beta/\rho_A^\alpha)$ with ΔA_V the Helmholtz free energy change and ΔS_V the entropy change of the composite system for the isochoric process. Then

$$\Delta A_V^* = \Delta U_V - T\Delta S_V^*. \tag{5}$$

The hydrophobicity in the constant-volume condition may be defined by the following condition analogous to eqn (4):

$$\Delta U_V < 0 \text{ and } T\Delta S_V^* < \Delta U_V, \tag{6}$$

which means that the forced accommodation of a solute in the solvent is energetically favorable but to a larger extent entropically unfavorable.

One might expect that in the thermodynamic limit whether the pressures are fixed or the volumes are fixed upon the transfer of a solute A has little consequence for the solvation thermodynamic quantities. However, that is not generally true as carefully discussed in earlier studies.[15–18] We illustrate this point for methane in water using experimental data in the following section, and then for the Lennard-Jones fluid mixtures in the main part.

Section 2 summarizes the thermodynamics of the constant-pressure and constant-volume solvation processes. In section 3 the simulation method including the free-energy calculation is described. In section 4 the numerical results for the solvation processes in the liquid mixtures are presented. We will see there that which of p and V is fixed in the solvation process has a profound effect on the manifestation of "hydrophobicity".

2. Constant-pressure and constant-volume solvations

Let $\mu_{ex,A}$ denote the excess chemical potential of species A defined by

$$\mu_{ex,A} = -kT\ln(\rho_A/z_A), \tag{7}$$

where z_A is the activity of A defined such that $z_A \to \rho_A$ as $\rho_A \to 0$. Then, for given thermodynamic states of phases α and β before (or after) the transfer of a molecule A,

$$\Delta A_V^* = \Delta G_p^* = \mu_{ex,A}^\beta - \mu_{ex,A}^\alpha = \Delta\mu_{ex}. \tag{8}$$

Note that the first equality is between ΔA^* for the constant-V process and ΔG^* for the constant-p process, which are both expressed as the difference in the excess chemical potential between the two phases.

The ratio ρ_A/z_A of the density to the activity, or equivalently $e^{-\mu_{ex,A}/kT}$, of each phase is given by the potential distribution theorem[19]

$$\frac{\rho_A}{z_A} = \langle e^{-\Psi/kT}\rangle \tag{9}$$

where Ψ is the interaction energy of molecule A fixed in space with the remaining molecules and the average $\langle\cdots\rangle$ is the canonical ensemble average in which the remaining molecules do not notice the existence of molecule A. Thus, in principle, one can calculate $\Delta\mu_{ex}$ by applying eqn (9) to the two phases. When the two phases are in equilibrium, $z_A^\alpha = z_A^\beta$ and so, from eqn (7)–(9), $\Delta\mu_{ex}$ is obtained from an experimentally measurable quantity $(\rho_A^\beta/\rho_A^\alpha)_{eq}$, the ratio of the equilibrium densities, as

$$\Delta\mu_{ex} = -kT\ln(\rho_A^\beta/\rho_A^\alpha)_{eq}. \tag{10}$$

In particular, when α is an ideal-gas phase of A ($\mu_{ex,A}^\alpha = 0$),

$$\mu_{ex,A}^\beta = -kT\ln(\rho_A^\beta/\rho_A^\alpha)_{eq}. \tag{11}$$

When $\Delta\mu_{ex}$ is decomposed into the energy (or enthalpy) and entropy changes as in eqn (3) or (5), each term is dependent on the process of transfer, *i.e.*, what is fixed before and after the transfer of a molecule A. The difference is given by

$$\frac{\Delta S_p^*}{k} - \frac{\Delta S_V^*}{k} = \frac{\Delta H_p}{kT} - \frac{\Delta U_V}{kT} = \frac{\varepsilon^\beta \bar{V}_A^\beta}{k\chi^\beta} - \frac{\varepsilon^\alpha \bar{V}_A^\alpha}{k\chi^\alpha}, \tag{12}$$

where ε and χ are, respectively, the coefficient of thermal expansion and the isothermal compressibility and $\bar{V}_A$ is the partial molar volume of a molecule A. The difference comes from the identity $(\partial X/\partial N_A)_{p,T} - (\partial X/\partial N_A)_{V,T} \equiv (\partial X/\partial V)_T \bar{V}_A$ for an arbitrary thermodynamic variable X of each phase.

As an illustration, consider a system consisting of a methane gas (phase α) and liquid water (phase β) at a pressure of 1 atm. As the temperature is increased from 0 to 100 °C, the Ostwald adsorption coefficient $(\rho_A^\beta/\rho_A^\alpha)_{eq}$ of methane in water decreases from 0.058 and then reaches a minimal value of 0.025 at around at around 80 °C.[20] The corresponding $\Delta\mu_{ex}$ of methane is given by eqn (10), which is positive and monotonically increases with the temperature in the range. The ΔS_p^* is then obtained from the identity

$$\frac{\Delta S_p^*}{k} \equiv -\frac{\partial\Delta\mu_{ex}}{\partial kT} + T(\varepsilon^\beta - \varepsilon^\alpha), \tag{13}$$

where the temperature differentiation is at fixed numbers of molecules of methane and water in each phase and at fixed pressure. However, when each phase is dilute in A, $\mu_{ex,A}$ of each phase is independent of the concentration ρ_A of A and so is $\Delta\mu_{ex}$. Thus, whether or not the number of molecules of methane is fixed in each phase does not change the temperature derivative of $\Delta\mu_{ex}$. So one can evaluate ΔS_p^* from the temperature dependence of $(\rho_A^\beta/\rho_A^\alpha)_{eq}$ at fixed pressure as

$$\frac{\Delta S_p^*}{k} = \frac{d}{dT}[T\ln(\rho_A^\beta/\rho_A^\beta)_{eq}] + T(\varepsilon^\beta - \varepsilon^\alpha). \tag{14}$$

With this and eqn (12), one can also evaluate ΔS_V^*.

Fig. 1 shows variations with the temperature of the solvation thermodynamic quantities for methane in water at atmospheric pressure. Plotted in Fig. 1a are $\Delta\mu_{ex}/kT$ and the decomposed elements. When $\Delta\mu_{ex}/kT$ is decomposed into the enthalpy change $\Delta H_p/kT$ and the excess entropy change $\Delta S_p^*/k$ for the process of transfer at fixed pressure, their variations over the temperature range are found to be much larger than that of $\Delta\mu_{ex}/kT$. At low temperatures near 0 °C, $\Delta H_p/kT$ and $\Delta S_p^*/k$ are both negative and large in magnitude; over the entire range of temperature they are nearly linear functions of T with nearly the same slope; and $\Delta H_p/kT$ changes sign at a temperature around 90 °C above which it is positive while $\Delta S_p/k$ is

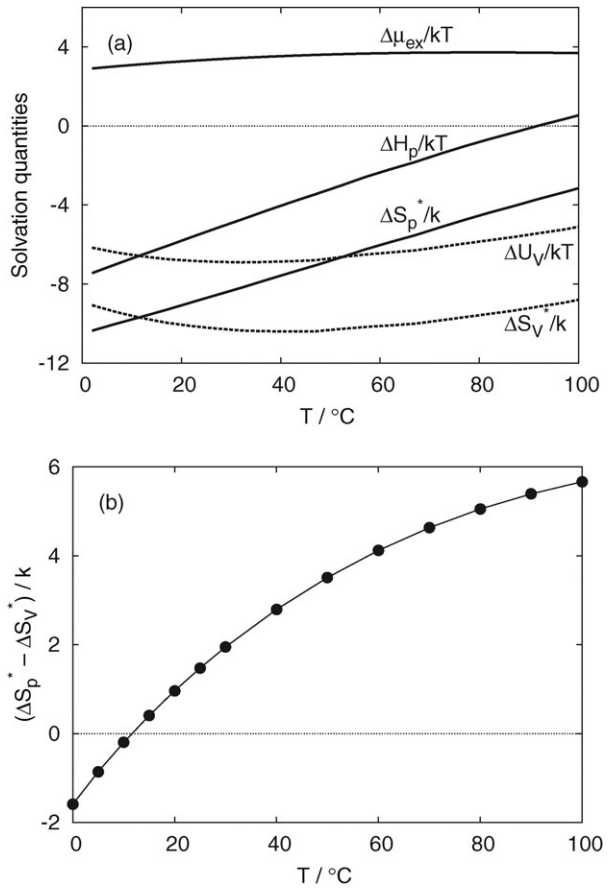

Fig. 1 Solvation thermodynamic quantities of methane in water as functions of temperature. The pressure is fixed at 1 atm. (a) $\Delta\mu_{ex}/kT$, $\Delta H_p/kT$, $\Delta S_p^*/k$, $\Delta H_V/kT$, $\Delta S_V^*/k$. (b) $(\Delta S_p^* - \Delta S_V^*)/k$, or equivalently $(\Delta H_p - \Delta U_V)/kT$.

negative. The last observation means that the constant-pressure transfer of the hydrophobic molecule from its gas phase to water at temperatures above 90 °C is unfavorable both energetically and entropically. The mechanism of low solubility there is different from that at low temperatures. Now consider the constant-volume solvation processes for the same equilibrium states at atmospheric pressure, that is, those in which the initial or the final state of the system is in two-phase equilibrium and the volume of each phase is fixed before and after the transfer. As shown by dashed lines in Fig. 1a, the energy change $\Delta U_V/kT$ and the excess entropy change $\Delta S_V^*/k$ are large and negative over the entire range of the temperature, and $\Delta S_V^*/k$ is larger in magnitude than $\Delta U_V/kT$. That is, the transfer with volume fixed is of hydrophobic character even when the one with pressure fixed is not. The difference $(\Delta S_p^* - \Delta S_V^*)/k$ is evaluated from eqn (12) with α being practically an ideal gas:

$$\varepsilon^\beta \bar{V}_A^\beta/k\chi^\beta - 1.$$

The coefficient of thermal expansion ε^β and the isothermal compressibility χ^β of water from 0 to 100 °C are taken from experimental data[21] and the partial molar volume of methane in water is assumed to be 36.2 cm^2 mol^{-1}.[22] The resulting $(\Delta S_p^* - \Delta S_V^*)/k$, or equivalently $(\Delta H_p - \Delta U_V)/kT$, is shown in Fig. 1b. It increases monotonically with the temperature from a negative value of −1.6 at 0 °C and changes it sign at around 10 °C where $\Delta S_p^* = \Delta S_V^*$. The change of the sign with the temperature variation is due to the coefficient of thermal expansion of water changing sign at 4 °C.

3. Solvation thermodynamics of Lennard-Jones mixtures

The model solutions we study here are Lennard-Jones mixtures consisting of 500 solvent particles and a solute particle A, all in a cubic box subject to periodic boundary conditions. With σ_0 and ε_0 the LJ size and energy parameters for pairs of solvent particles, temperature, pressure, and density are given by $T^\star = kT/\varepsilon_0$, $p^\star = p\sigma_0^3/\varepsilon_0$, and $\rho^\star = \rho\sigma_0^3$, and the solute–solvent LJ interaction parameters are given by $\sigma^\star = \sigma/\sigma_0$ and $\varepsilon^\star = \varepsilon/\varepsilon_0$, where superscripts ★ (not *) indicate that quantities are in the LJ units. The LJ potential functions, both between solvent particles and between solvent and solute particles, are truncated at half the dimension of the simulation cell. The long-range corrections to thermodynamic quantities are made by the standard procedure.

The solvation free energy $\Delta\mu_{ex}$ and other quantities of interest are obtained as functions of $\sigma^\star$ and $\varepsilon^\star$. The MC simulations described below are performed for sets of parameters $(\sigma^\star,\varepsilon^\star)$ in the range $0.8 \le \sigma^\star \le 2.0$ with an interval of 0.1 and in the range $0 < \varepsilon^\star \le 1.0$ with 11 points. The corresponding solute size would be in a range from 0.6 to 3.0 should it be evaluated by the Lorentz–Berthelot rule. The gas phase from which A is transferred to the solvent is taken to be ideal so that $\Delta\mu_{ex} = \mu_{ex,A}^\beta$.

Numerical evaluation of $\Delta\mu_{ex}$ is done by the thermodynamic integration method,[23] where the MC simulations are performed for the systems with the potential

$$\Psi(\lambda) = \Psi_0 + \lambda^n\Psi_A, \qquad (15)$$

where Ψ_0 is the potential energy due to all the interactions among solvent molecules and Ψ_A is the potential energy due to the interactions between a solute molecule A and all the solvent molecules; λ is a coupling parameter ranging from 0 to 1 and n is in practice taken to be greater than 1. The excess chemical potential is then given by

$$\Delta\mu_{ex} = n\int_0^1\langle\lambda^{n-1}\Psi_A\rangle_\lambda\, d\lambda, \qquad (16)$$

where $\langle\cdots\rangle_\lambda$ denotes the average with the potential $\Psi(\lambda)$. This formula is independent of the choice of ensembles; either the canonical (NVT) or the isothermal–isobaric (NpT) MC simulation can be employed. The Widom particle insertion method, another standard method, was also employed for solvation of small solutes, and we confirmed that the results agree with those obtained from the thermodynamic integration method. For large solutes, however, the particle insertion method becomes impractical, and so the thermodynamic integration method is used for all sets of potential parameters.

Numerical calculations of eqn (16) were carried out as follows. The power n is set to 5 and the increment of λ to 0.05. Equilibrium configurations are generated by the canonical MC and isothermal–isobaric MC simulations. The

thermodynamic states examined are $p^\star = 0.12$, $T^\star = 0.7$ (close to the triple point) and $p^\star = 1.13$, $T^\star = 0.7$; the corresponding densities of solvent particles when the solute A is absent at those states are $\rho^\star = 0.8507$ and 0.900, and these values are used as the input in the canonical MC simulations. The number of MC steps at each thermodynamic state is 8 million for the canonical simulation and 25 to 65 million for the isothermal–isobaric simulation. The average $\langle\cdots\rangle_\lambda$ in eqn (16) is obtained from the above MC runs excluding the first 50 thousand steps for equilibration and is numerically integrated to give $\Delta\mu_{ex}$.

The enthalpy of transfer is

$$\Delta H_p = (\partial H^\beta/\partial N_A)_{p,T} - (\partial H^\alpha/\partial N_A)_{p,T}. \quad (17)$$

The first term is evaluated as enthalpy difference between the system (phase β) with and without solute A at a common pressure, which is obtained from the constant-NpT MC simulations at $\lambda = 1$ (the system with a solute A) and $\lambda = 0$ (the system without A). The second term is simply kT, for α is an ideal gas. The energy of transfer is

$$\Delta U_V = (\partial U^\beta/\partial N_A)_{V,T} - (\partial U^\alpha/\partial N_A)_{V,T}. \quad (18)$$

Again, the first term is evaluated as the difference in energy between the system (phase β) with and without solute A at a common volume, which is obtained from the canonical MC simulation. The second term is zero, for α is an ideal gas.

Fig. 2 shows the constant-pressure solvation diagram in the $\sigma^\star$,$\varepsilon^\star$ plane, which indicates regions of low solubility ($\Delta\mu_{ex} > 0$), high solubility ($\Delta\mu_{ex} < 0$), endothermic solvation ($\Delta H_p > 0$), and exothermic solvation ($\Delta H_p < 0$). In the case of $p^\star = 0.12$ as shown in Fig. 2a, the domain of $\Delta\mu_{ex} > 0$ and that of $\Delta H_p > 0$ largely overlap each other, occupying large $\sigma^\star$ and $\varepsilon < 1$ regions. There is, however, a narrow region (a shaded area in the figure) in which $\Delta\mu_{ex} > 0$ and $\Delta H_p < 0$, *i.e.*, the solvation has the essential character of hydrophobicity. That region is found where $\sigma^\star < 1$ and $\varepsilon^\star < 0.7$. That is, the necessary condition that an LJ solute particle in LJ solvent particles be 'hydrophobic' is that the size of the solute particle must be smaller than that of the solvent particles and the strength of solute–solvent intermolecular interaction is smaller than that of solvent–solvent ones. Solvation of various inert gases in organic liquids shows a tendency that as the size of solute species decreases the solvation free energy $\Delta\mu_{ex}$ increases and becomes positive while ΔH_p remains negative.[24] This observation is consistent with the result presented here for the LJ mixtures. Effects of the pressure is seen from comparison of Fig. 2a with Fig. 2b. The analogue of the hydrophobic hydration manifests itself in a wider region of the $\sigma^\star$,$\varepsilon^\star$ parameter space at the higher pressure.

For the constant-volume solvation, regions of positive and negative ΔU_V as well as those of $\Delta\mu_{ex}$ in the $\sigma^\star$,$\varepsilon^\star$ plane are displayed in Fig. 3. In the parameter space examined, the constant-volume solvation is exothermic ($\Delta U_V < 0$) except in the cases that the solute–solvent interaction parameter $\varepsilon^\star$ is very small; on the other hand, the region of $\Delta\mu_{ex} > 0$ is the same as the one under the constant-pressure condition as it should be. Thus the low solubility with exothermic character

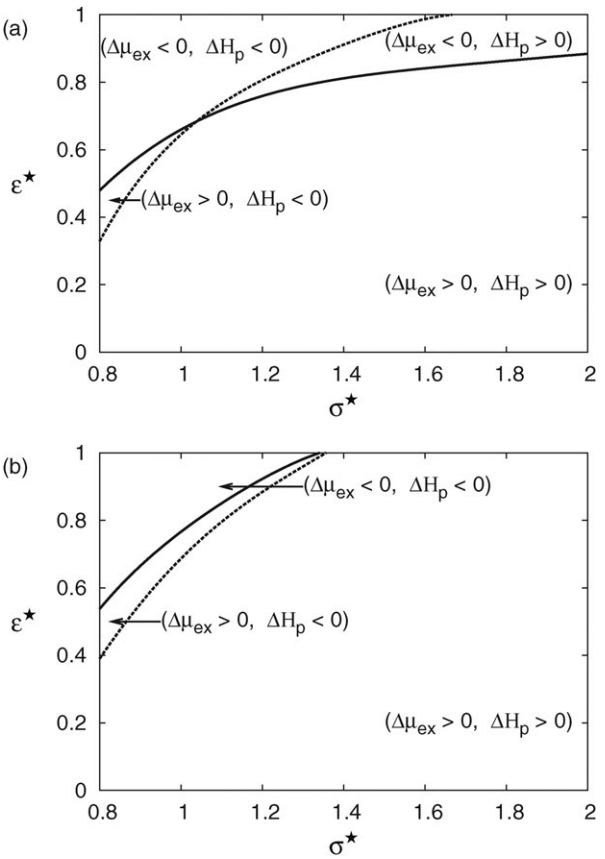

Fig. 2 Constant-pressure solvation diagram. (a) $p^\star = 0.12$, $T^\star = 0.7$ (a state close to the triple point); (b) $p^\star = 1.13$, $T^\star = 0.7$ (a high-pressure state).

($\Delta\mu_{ex} > 0$ and $\Delta U_V < 0$) under the fixed-volume condition is observed in a wide range of the solute–solvent LJ parameter space, in contrast to the one in the fixed-pressure condition. As the solvent density is increased (Fig. 3b), the borders $\Delta U_V = 0$ and $\Delta\mu_{ex} = 0$ are shifted to the direction of large $\varepsilon^\star$.

Contours of constant $\Delta\mu_{ex}$ at $p^\star = 0.12$ obtained from the canonical ensemble MC simulations are shown in Fig. 4. The corresponding contours obtained from the isothermal–isobaric MC simulations were very similar to these, which supports the numerical accuracy of the free-energy calculations. (Minor discrepancies are seen at large values of $\sigma^\star$ where the finite-size effect in the simulation becomes noticeable.) Broadly speaking, $\Delta\mu_{ex}$ is large at large $\sigma^\star$ and small $\varepsilon^\star$ and it is small at small $\sigma^\star$ and large $\varepsilon^\star$, as anticipated. When the solute particle is identical with the solvent particles, *i.e.*, $\sigma^\star = 1$ and $\varepsilon^\star = 1$, $\Delta\mu_{ex}$ is negative. As $\varepsilon^\star$ is decreased with $\sigma^\star$ being fixed at 1, $\Delta\mu_{ex}$ increases and reaches a maximum positive value at $\varepsilon^\star \simeq 0.1$, and then as $\varepsilon^\star$ goes to 0, it rapidly decreases and approaches 0, as it should. Note that a branch of contours of $\Delta\mu_{ex} = 0$ is the line of $\varepsilon^\star = 0$ (as indicated by label "0" on the $\sigma^\star$ axis in Fig. 4), for the solute with $\varepsilon^\star = 0$ is non-interacting.

For the constant-pressure solvation process, $\Delta\mu_{ex}$ is decomposed to ΔH_p and $-T\Delta S_p^*$. To see their variations in the $\sigma^\star$, $\varepsilon^\star$ plane, contours of constant ΔH_p and those of constant $T\Delta S_p^*$ are plotted and displayed in Fig. 5a and b,

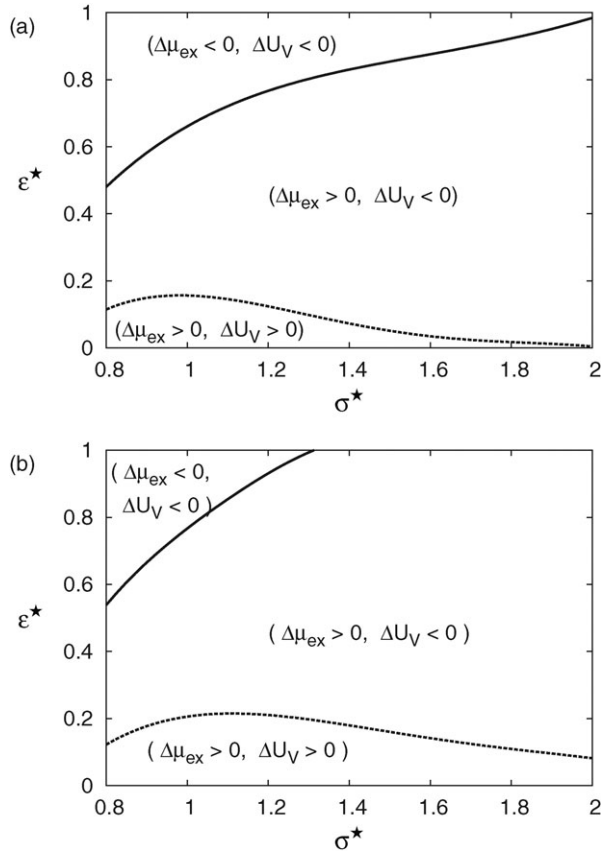

Fig. 3 Constant-volume solvation diagram. (a) $\rho^\star = 0.8507$, $T^\star = 0.7$ ($p^\star = 0.12$, a state close to the triple point); (b) $\rho^\star = 0.9000$, $T^\star = 0.7$ ($p^\star = 1.13$, a high-pressure state).

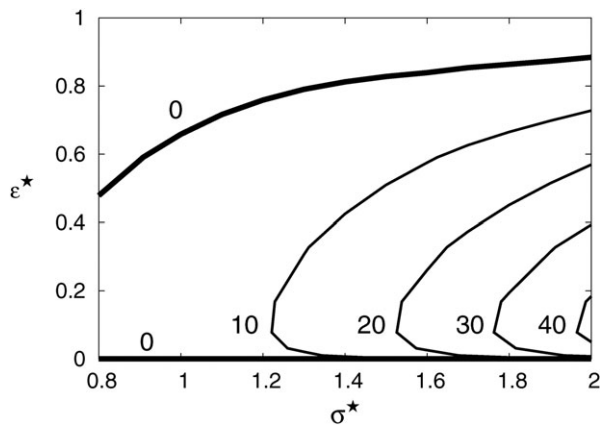

Fig. 4 Contours of constant $\Delta\mu_{ex}$ at $p^\star = 0.12$, $T^\star = 0.7$. The number for each contour is the value of $\Delta\mu_{ex}$ in units of ε_0.

respectively. It is seen that the variation of ΔH_p is similar to that of $\Delta\mu_{ex}$. The value of ΔH_p is large and positive when $\sigma^\star$ is large and $\varepsilon^\star$ is moderately small while it is negative at small $\sigma^\star$ and large $\varepsilon^\star$. Variation of $T\Delta S_p^*$ in the $\sigma^\star$,$\varepsilon^\star$ plane is similar to that of ΔH_p. ΔS_p^* is large and positive when $\sigma^\star$ is large and $\varepsilon^\star$ is small (but not too small). Now we note that $\Delta S_p^* = (\partial S_{ex}^\beta/\partial N_A)_{p,T} - (\partial S_{ex}^\beta/\partial N_A)_{p,T}$, where $S_{ex} = S(\rho_A) - S_{id}(\rho_A)$; and $S_{ex}^\alpha = 0$, for α is an ideal gas.

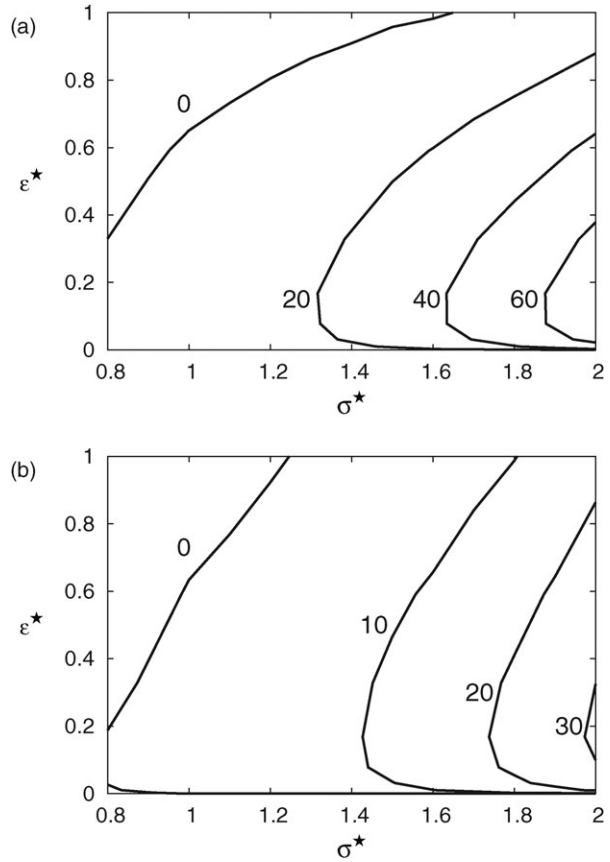

Fig. 5 (a) Contours of constant ΔH_p and (b) contours of constant $T\Delta S_p^*$. All the values in the figures are in units of ε_0.

So $\Delta S_p^* = (\partial S_{ex}^\beta/\partial N_A)_{p,T}$, which is the solvation entropy of phase β arising from the existence of solute A fixed in a space. The microscopic expression for ΔS_p^* is then

$$\Delta S_p^* = k \ln[W_A(U_A)/W(U)], \qquad (19)$$

i.e., the logarithm of the ratio of the number $W_A(U_A)$ of accessible states for the system with a solute particle A fixed in space to the corresponding number $W(U)$ for the system of solvent particles alone, both under a common pressure. U_A and U are the average energies of the system with and without the solute particle at the common pressure. When the solute is identical to the solvent ($\sigma^\star = 1$ and $\varepsilon^\star = 1$), $\Delta S_p^* < 0$, in agreement with experimental observation that the solvation entropies of inert gases in their own liquids are negative.[25] In order for a solute particle of the same size as a solvent particle ($\sigma^\star = 1$) to have $\Delta S_p^* = 0$, the solute–solvent interaction must be weaker than the solvent–solvent interaction ($\varepsilon^\star \simeq 0.6$).

In the constant-volume solvation process, $\Delta\mu_{ex}$ is decomposed to ΔU_V and $-T\Delta S_V^*$. The contours of constant ΔU_V are qualitatively different from those of constant ΔH_p. As shown in Fig. 6a, ΔU_V is negative except at small values of $\varepsilon^\star$, in contrast to ΔH_p which is positive in a major part of the examined parameter space, and ΔU_V becomes increasingly negative as $\varepsilon^\star$ and $\sigma^\star$ increase. Likewise, variation of $T\Delta S_V^*$ is strikingly different from that of $T\Delta S_p^*$: compare Fig. 6b with Fig. 5b. First, in contrast to ΔS_V^* being negative

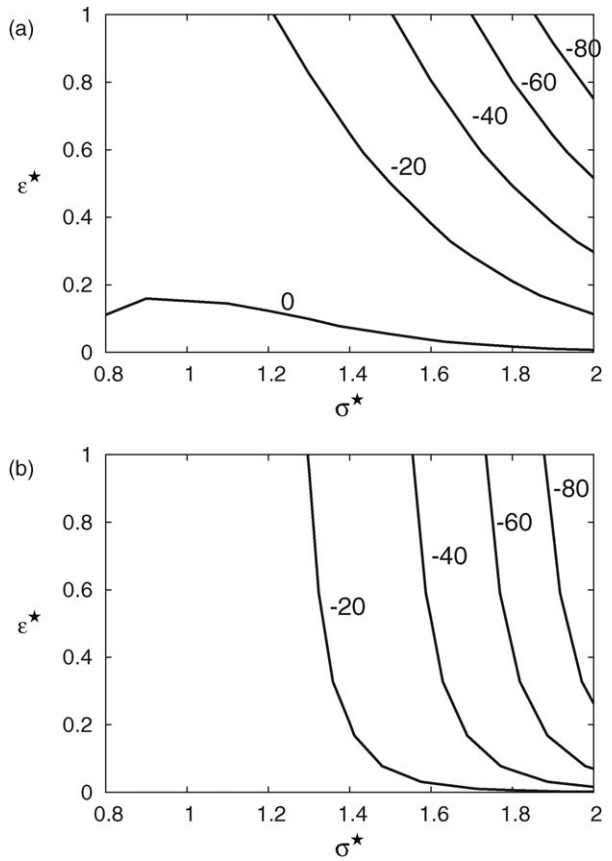

Fig. 6 (a) Contours of constant ΔU_V and (b) contours of constant $T\Delta S_V^*$. All the values in the figures are in units of ε_0.

for any set of $\sigma^\star$ and $\varepsilon^\star$ in the examined ranges, ΔS_p^* is positive for wide ranges of the LJ parameters. Second, ΔS_V^* decreases, *i.e.*, becomes more negative, with increasing $\sigma^\star$ at fixed $\varepsilon^\star$ while ΔS_p^* increases and becomes more positive as $\sigma^\star$ increases from 0.8 to 2 at fixed values of $\varepsilon^\star < 1$.

As illustrations of "hydrophobic" and "hydrophilic" solutes, let us examine two solute species, A and B, with the following LJ parameters: (A) $\sigma^\star = 0.9$, $\varepsilon^\star = 0.54$; (B) $\sigma^\star = 1.0$, $\varepsilon^\star = 0.5$. We calculate $\Delta\mu_{ex,A}$ and $\Delta\mu_{ex,B}$ over a temperature range from $T^\star = 0.6$ to 1.2 at $p^\star = 0.12$. In the diagram in Fig. 2a, the LJ parameter set of species A is in the narrow region in which $\Delta\mu_{ex,A} > 0$ and $\Delta H_p < 0$, *i.e.*, the solvation is of hydrophobic character, and the parameter set of species B is outside that narrow region, where ΔH_p is now positive. The calculated $\Delta\mu_{ex,A}/kT$ and $\Delta\mu_{ex,B}/kT$ are both positive in the temperature range, *i.e.*, the solubility of these solute species in the solvent is low; but their temperature dependences contrast markedly with each other. Fig. 7 shows the variation of $\Delta\mu_{ex,A}/kT$ with temperature, where one can see that $\Delta\mu_{ex,A}/kT$ increases with $T^\star$ until it reaches its maximum value at around $T^\star = 0.8$, *i.e.*, the solubility of the LJ solute A in the LJ solvent decreases with increasing temperature in the low-temperature range and then turns to increase. This temperature dependence of $\Delta\mu_{ex,A}/kT$ is qualitatively the same as that characterizing the hydrophobic hydration. In contrast, $\Delta\mu_{ex,B}/kT$ decreases monotonically with increasing the temperature, *i.e.*, the solubility increases with temperature.

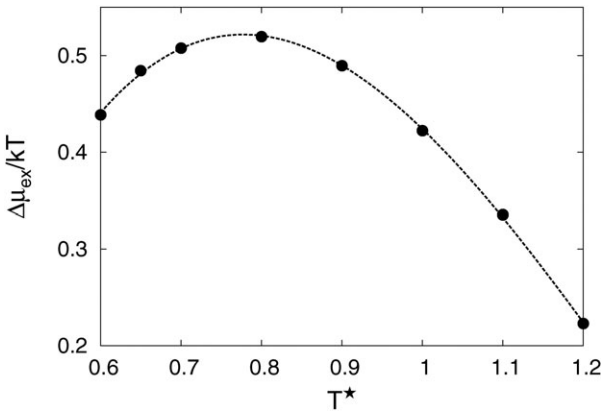

Fig. 7 Variation of $\Delta\mu_{ex,A}/kT$ with $T^\star$. The solute–solvent LJ parameters are $\sigma^\star = 0.9$, $\varepsilon^\star = 0.54$. Dashed curve is a cubic fit to the corresponding data points.

The results for species A and B are consistent with the signs of their ΔH_p's at $T^\star = 0.7$.

From the constant-NpT MC simulations for obtaining $\Delta\mu_{ex,A}$ at each temperature, we also evaluated ΔH_p directly, and then obtained ΔS_p^* from $\Delta\mu_{ex,A}$ and ΔH_p. Fig. 8 shows their variations with temperature: the solvation of species A is such that $\Delta H_p < 0$ *but* $\Delta\mu_{ex,A} > 0$ at low temperatures because $T\Delta S_p^*$ is even more negative than ΔH_p while at high temperatures $\Delta H_p > 0$ *and* $\Delta\mu_{ex,A} > 0$. That is, both ΔH_p and ΔS_p^* change their signs as $T^\star$ is varied in the range. Statistical uncertainties in data points of $\Delta H_p/kT$ and $\Delta S_p^*/k$ are within ± 0.2, and those of $\Delta\mu_{ex,A}/kT$ are within the size of data points.

Temperature dependences of $\Delta\mu_{ex,A}$ and $\Delta\mu_{ex,B}$ are calculated also for the constant volume condition. When the density is fixed to $\rho^\star = 0.8507$, the value at $T^\star = 0.7$ and $p^\star = 0.12$, both $\Delta\mu_{ex,A}/kT$ and $\Delta\mu_{ex,B}/kT$ increase monotonically with increasing $T^\star$. This result, too, is consistent with the diagram in Fig. 3, for the LJ parameter sets for species A and B are both in the "hydrophobic" region in the constant-volume diagram.

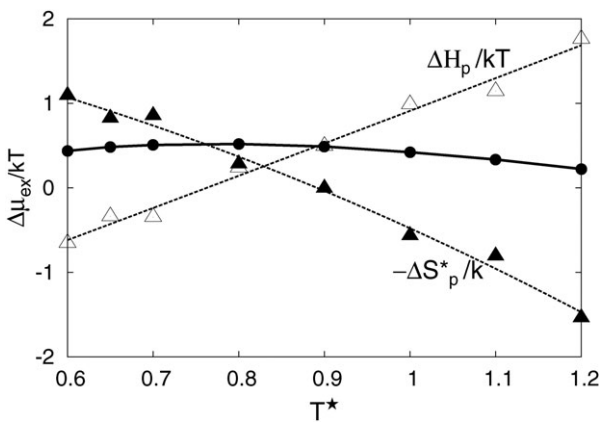

Fig. 8 Variations of $\Delta H_p/kT$ and $-\Delta S_p^*/k$ with $T^\star$, together with that of $\Delta\mu_{ex,A}/kT$. The solute–solvent LJ parameters are the same as in Fig. 7. Dashed curves are parabolic fits to the corresponding data points.

Finally we note that, although so far ΔH_p and ΔU_V have been evaluated directly from the MC simulations, one may use eqn (12) with α being an ideal gas:

$$\Delta H_p - \Delta U_V = kT\left[\frac{\varepsilon^\beta \bar{V}_A^\beta}{k\chi^\beta} - 1\right] \tag{20}$$

Among these quantities, the ratio $\varepsilon^\beta/\chi^\beta$, a property of the solvent, is obtained from an accurate equation of state for the LJ liquid[26] through the thermodynamic identity:

$$\frac{\varepsilon^\beta}{\chi^\beta} = \left(\frac{\partial p}{\partial T}\right)_\rho. \tag{21}$$

The partial molar volume $\bar{V}_A^\beta$ of solute A in phase β is given by

$$\bar{V}_A^\beta = \left(\frac{\partial \Delta\mu_{ex}}{\partial p}\right)_T + kT\chi^\beta \tag{22}$$

with χ^β given by the equation of state and the pressure derivative of $\Delta\mu_{ex}$ approximated to be $[\Delta\mu_{ex}(p+\Delta p) - \Delta\mu_{ex}(p)]/\Delta p$ and evaluated from simulations at different pressures. At $T^\star = 0.7$ and $p^\star = 0.12$, we find

$$\Delta H_p - \Delta U_V = 3.6, \text{ direct}$$

$$\Delta H_p - \Delta U_V = 5.9, \text{ indirect}$$

where the values are in units of ε_0. The first result is from direct evaluation of ΔH_p and ΔU_V from the NpT and NVT MC simulations and the second one is from eqn (20) with eqn (21) and (22). The two do not agree very well. It is mainly due to the statistical errors in evaluating $\bar{V}_A^\beta$ from the two methods: $\bar{V}_A^\beta = 1.5$ from eqn (22) while $\bar{V}_A^\beta = 0.8$ from the NpT simulations with and without solute A in phase β.

4. Summary

In order to learn about the general features of the hydrophobic hydration, we studied a model of simple liquids, namely, the LJ solution. An essential feature of hydrophobicity is that the solvation is energetically favorable but is entropically more unfavorable in magnitude, as expressed by eqn (4) or (6). But the entropic contribution to the solvation free energy $\Delta\mu_{ex}$ [eqn (8)] for transferring a solute from an ideal-gas phase α to a solvent phase β depends on the thermodynamic condition, *i.e.*, whether the pressures are fixed or the volumes are fixed for the two phases.

This point was illustrated for the solvation of methane in water. If the constant-pressure solvation is assumed, ΔH_p becomes less negative, *i.e.*, the solvation becomes less exothermic as temperature increases and the solvation becomes energetically and entropically unfavorable at high temperatures. On the other hand, if the constant-volume solvation is assumed, the solvation is of hydrophobic character over the entire temperature range. The difference $\Delta S_p^* - \Delta S_V^*$ changes its sign at around 10 °C because the coefficient of thermal expansion of water changes its sign at 4 °C.

For estimation of $\Delta S_p^* - \Delta S_V^*$, or $\Delta H_p - \Delta U_V$, for the solvation of more complex solutes, *e.g.*, proteins, in solutions, one must have an access to the partial molar volume of such solutes as well as the coefficient of thermal expansion and the compressibility of solutions. Experimental data of those quantities are much needed.

For the LJ solution, we identified the solute–solvent LJ parameters for which the solvation is of hydrophobic character. For the isobaric solvation process, in the $\sigma^\star$,$\varepsilon^\star$ plane there is a narrow region of small $\sigma^\star$ and small $\varepsilon^\star$ in which $\Delta\mu_{ex} > 0$ and $\Delta H_p < 0$, *i.e.*, the solvation is analogous to the hydrophobic hydration. For the isochoric process, in the same parameter space, there is a wide "hydrophobic" region in which $\Delta\mu_{ex} > 0$ and $\Delta U_V < 0$. The difference between the two processes also manifests itself in the contrast between ΔH_p and ΔU_V in the $\sigma^\star$,$\varepsilon^\star$ plane (Fig. 5a and 6a) and in the contrast between ΔS_p^* and ΔS_V^* (Fig. 5b and 6b).

Acknowledgements

We thank Professor B. Widom for insightful discussions. This work was supported by Grant-in-Aid for Scientific Research and the Next Generation Super Computing Project from MEXT, Japan.

References

1 I. Ohmine and H. Tanaka, *Chem. Rev.*, 1993, **93**, 2545–2566.
2 F. Franks, *Water: A Matrix of Life*, Royal Society of Chemistry, Cambridge, 2nd edn, 2000.
3 P. Ball, *Life's matrix: a biography of water*, Farrar, Straus and Giroux, New York, 1st edn, 2000.
4 B. Guillot and Y. Guissani, *J. Chem. Phys.*, 1993, **99**, 8075–8094.
5 S. Shimizu and H. S. Chan, *J. Chem. Phys.*, 2000, **113**, 4683–4700.
6 L. R. Pratt and D. Chandler, *J. Chem. Phys.*, 1977, **67**, 3683–3704.
7 K. A. T. Silverstein, A. D. J. Haymet and K. A. Dill, *J. Am. Chem. Soc.*, 1998, **120**, 3166–3175.
8 A. B. Kolomeisky and B. Widom, *Faraday Discuss.*, 1999, **112**, 81–89.
9 A. Ben-Naim, *Hydrophobic Interactions*, Plenum Press, Oxford, 1980.
10 H. S. Frank and M. W. Evans, *J. Chem. Phys.*, 1945, **13**, 507–532.
11 G. Hummer, S. Garde, A. E. García and L. R. Pratt, *Chem. Phys.*, 2000, **258**, 349–370.
12 S. V. Buldyrev, P. Kumar, P. G. Debenedetti, P. J. Rossky and H. E. Stanley, *Proc. Natl. Acad. Sci. U. S. A.*, 2007, **104**, 20177–20182.
13 A. Ben-Naim, *J. Chem. Phys.*, 2008, **129**, 104506.
14 A. Ben-Naim and S. V. K., *J. Chem. Phys.*, 2008, **129**, 194514.
15 N. Matubayasi, L. H. Reed and R. M. Levy, *J. Phys. Chem.*, 1994, **98**, 10640–10649.
16 D. Ben-Amotz and B. Widom, *J. Phys. Chem. B*, 2006, **110**, 19839–19849.
17 M. Kinoshita, Y. Harano and R. Akiyama, *J. Chem. Phys.*, 2006, **125**, 244504.
18 P. De Gregorio and B. Widom, *J. Phys. Chem. C*, 2007, **111**, 16060–16069.
19 B. Widom, *J. Chem. Phys.*, 1963, **39**, 2808–2812.
20 R. Battino, *IUPAC Solubility Data Series*, Pergamon, Oxford, 1987, vol. 27/28, pp. 1–6.
21 R. A. Fine and F. J. Millero, *J. Chem. Phys.*, 1973, **59**, 5529–5536.
22 A. Ben-Naim, in *Solvation Thermodynamics*, Plenum Press, New York, 1987, ch. 2, p. 73.
23 M. Mezei and D. L. Beveridge, *Ann. N. Y. Acad. Sci.*, 1986, **482**, 1.
24 A. Ben-Naim, in *Solvation Thermodynamics*, Plenum Press, New York, 1987, ch. 2, p. 66.
25 A. Ben-Naim, in *Solvation Thermodynamics*, Plenum Press, New York, 1987, ch. 2, p. 52.
26 J. K. Johnson, J. A. Zollweg and K. E. Gubbins, *Mol. Phys.*, 1993, **78**, 591.